

ANANTHAKUMAR
SUDALAIMANI¹
BARATHIRAJA RAJENDRAN²
THIYAGARAJ JOTHI³
ASHOKKUMAR
MOHANKUMAR⁴

¹Department of Mechanical
Engineering, Government
College of Engineering,
Tirunelveli, Tamil Nadu, India

²Department of Mechanical
Engineering, Einstein College of
Engineering, Near MS
University, Tirunelveli, Tamil
Nadu, India

³Department of Mechatronics
Engineering, Er. Perumal
Manimekalai College of
Engineering, Hosur, Tamil Nadu,
India

⁴Department of Mechanical
Engineering, Government
College of Engineering, Bargur,
Krishnagiri, Tamil Nadu, India

SCIENTIFIC PAPER

UDC 66:665.3:620

EFFECTS OF EXHAUST GAS RECIRCULATION ON DIESEL ENGINE USING HYBRID BIODIESEL

Article Highlights

- Diesel engines may run on hybrid blends up to 100% without any changes
- EGR rates and appropriate hybrid mixes can solve the smoke/NO_x trade-off
- With the addition of WPO to the engine, engine performance is marginally reduced
- Up to a specific load range, CO emissions may be regulated; after that, they start to grow.

Abstract

The primary aim of this study is to alternate between conventional fossil fuels and reduce the emissions of greenhouse gases and sulfur dioxide from diesel engines. In the current study, to mitigate NO_x emissions, the exhaust gas recirculation (EGR) technique was implemented utilizing hybrid alternate biodiesel at three varying proportions of 5%, 10%, and 15% at an optimum compression ratio of 20:1. The findings demonstrate that for hybrid alternative biodiesel at a compression ratio of 20:1 and fully loaded, the brake thermal efficiency (BTHE) is 31.8% with 10% EGR. With 15% EGR, the peak pressure for the hybrid biodiesel is lower than it would be without EGR by around 2.28%. When EGR is increased, the ignition delay and NO_x emissions are reduced slightly. With only an increase in EGR rates of up to 10%, brake-specific fuel consumption (BSFC) values were reduced efficiently. The hybrid biodiesel with 10% EGR reduces exhaust gas temperature to 341 °C.

Keywords: exhaust gas recirculation, combustion, performance, emission, waste plastic oil; rubber seed oil.

Biofuels encompass various alternative fuels, including biogas, producer gas, natural gas, hydrogen, alcohol, and vegetable oils. However, among these options, biodiesel is a desirable substitute for the auto-

mobile industry, particularly in diesel engines. Biodiesel is the most versatile energy source, contributing to approximately 10% of global energy consumption. This renewable fuel has transitioned into a modern, globally traded product, making significant strides in the automotive and electricity sectors. Energy independence and climate change mitigation are the two main drivers of biodiesel development. Biodiesel is the most feasible and sustainable option for replacing gasoline and diesel in isolation or as blends with petroleum-based fuels. Using liquid biodiesel for transportation is a vital strategy to enhance fuel security, foster rural development, and create employ-

Correspondence: B. Rajendran, Department of Mechanical Engineering, Einstein College of Engineering, Near MS University, Tirunelveli - 627 012, Tamil Nadu, India.

E-mail: barathiraja.r@einsteincollege.ac.in

Paper received: 3 March, 2023

Paper revised: 3 August, 2023

Paper accepted: 23 August, 2023

<https://doi.org/10.2298/CICEQ230303022A>

ment opportunities for individuals worldwide.

Biodiesel is made from vegetable oil and usually works in diesel engines run on diesel fuel [20]. Enzymes can be used as catalysts in biodiesel production using sustainable feedstocks. Research on innovative and sustainable biodiesel production technologies to boost output and improve performance might be necessary for competitive biodiesel. Biodiesel is less expensive than fossil fuel, renewable, nontoxic, and doesn't cause global warming. Also, due to the abundance of plastic waste and its potential for use as energy, scholars are very interested in the pyrolysis of plastic waste to reduce pollution and energy crises. Several studies have looked into using plastic oil as an alternative fuel. Waste plastic oil (WPO) may be used for internal combustion engines since it has similar heating values, density, and cetane index to diesel fuel [1]. The literature further suggests that diesel engines may achieve comparable performance, stability, and efficiency by using waste plastic oil [2]. Rafael *et al.* [3] raised the main issues concerning the recent development of plastic-added biodiesel and its blend characteristics, fuel qualities, combustion quality, and environmental impact. Damodharan *et al.* [4] looked into the separation and analysis of WPO from the catalytic pyrolysis process. It helped them determine what the oxygenated *n*-butanol (B) component looks like. The blends D50-WPO30-B20, D50-WPO40-B10, and D50-WCO20-B30 are used as fuels. The B10 blend reduces NO_x emissions compared to WPO and diesel. However, compared to WPO, the B30 mix emits more NO_x. As the *n*-butanol proportion in the mix rises, brake thermal efficiency (BTE) and fuel usage improve. For compression ignition (CI) engines that work well with WPO, *n*-butanol could be a feasible additive.

Using WPO mixes in a CI engine, Sachin *et al.* [5] analyzed the performance and emission characteristics. It has been shown that WPO mixes have a lower BTE and a higher brake-specific fuel consumption (BSFC) and exhaust gas temperature. The NO_x and CO emissions increase, but the hydrocarbon emissions decrease with an increase in WPO blends. WPO is tested in a CI engine, and its performance parameters were investigated by Mani *et al.* [6]. According to reports, an engine running at 100% WPO emits more NO_x, CO, hydrocarbons (HC), and smoke than a diesel engine. Furthermore, the exhaust gas temperature is higher, and the BTE is higher up to 80% of the load.

Recent studies have been performed on the combustion and operative parameters of a CI engine running on hybrid alternative mixtures, such as canola oil and waste palm oil [7], *Jatropha* and soap nut oils

[8], methyl ester of paradise and eucalyptus oil [9], palm and *Calophyllum inophyllum* oil [10], hazelnut soap stock and waste sunflower oil [11], palm and coconut biodiesel blend [12], pal and *jatropha* biodiesels with additives [13], and sunflower and cottonseed oil methyl esters [14].

Habibullah *et al.* [12] studied the effects of a palm and coconut biodiesel mix (PB20, CB20, PB15CB5, PB10CB10, and PB5CB15) in a CI engine. Higher reductions in BTE, increased BSFC, and NO_x emissions are observed for the CB20 blend compared with the PB20 blend. Whereas combined blends reduced NO_x emissions and improved BTE and BSFC. The characteristics of blends containing waste sunflower oil and hazelnut soap stock at 5%, 10%, 15%, 17.5%, and 25% were evaluated by Usta *et al.* [11]. The results indicated that a 17.5% blend had the highest BTHE; however, all mixes had greater NO_x, CO, and exhaust temperatures than diesel fuel. Performances and emissions of a compression ignition engine operated on a combination of palm and *Calophyllum inophyllum* oil were assessed by Ashrafur *et al.* [10]. Both biodiesel and diesel mixes exhibit higher BSFC and lower EGT than diesel. For higher blends, NO_x emissions increase, whereas CO and HC emissions decrease.

One of the most effective, versatile, and dependable emission reduction solutions for decreasing NO_x emissions is exhaust gas recirculation (EGR). The following modifications take place during diesel engine combustion when EGR percentages rise: (i) a higher specific heat capacity, which lowers both the chamber and localized flame temperatures; (ii) a longer flame expansion due to a lower inlet oxygen content, which lowers the local temperature. (iii) When H₂O and CO₂ are cycled, an endothermic disintegration process begins, lowering the flame temperatures [15]. The EGR hydrogen engine was suggested by Ming *et al.* [16] after reviewing the usage of EGR and its effects on diesel engines. Several studies have recently examined the combustion and performance of the CI engine running on biodiesel at various EGR rates, such as soybean biodiesel [17], mahua methyl ester [18], WPO [19], rubber seed oil blends [20], rapeseed methyl ester blends [21], *jatropha* blends [22], *n*-pentanol blends [23], cotton seed biodiesel blends [24], soybean oil [25], jojoba oil [26], waste apple seeds [27], and chicken wastes [28].

Mani *et al.* [19] inspected the consequences of cooled EGR in a CI engine operated with clean WPO. The results showed that NO_x discharges are higher without EGR but up to 20% lower with cooled EGR. Additionally, it has been shown that 20% cooled EGR emits less smoke, CO, and HC. In a CI engine with a

cooled EGR, Ramadhas *et al.* [20] inspected the emission and performance parameters of rapeseed oil (RSO) mixes. Due to the reduced temperature in the combustible chamber, the emissions of NO_x were also decreased. The BTE of the CI engine increases with EGR. While the emissions of HC and CO rise, the opacity of the smoke remains constant.

Saleh [26] investigated the impact of recirculation of exhaust gases (5–15%) on a CI engine running on biodiesel made from jojoba. The outcomes demonstrated an improved interchange between NO_x, HC, and CO releases with an EGR of 5%–15% when NO_x emissions were reduced. Rajesh and Saravanan [23] investigated the efficiency and exhaust releases of a CI engine running on several n-pentanol blends of 10, 20, 30, and 45% with varying levels of recirculation of exhaust gas (10%, 20%, and 30%). The findings demonstrated that NO_x emissions should be reduced by increasing EGR rates for a 45% blend. However, smoke opacity hardly increased. Further, hydrocarbons and carbon monoxide emissions are observed to be increased for all EGR conditions. Srinivasa [24] experimentally investigated a CI engine running on a mix of biodiesel made from cotton seeds (10%, 20%, and 30%) with various EGRs of 0%, 5%, 10%, 15%, and 20%. The reduction in NO_x emissions is observed for all blends with 15% EGR compared to other EGR rates.

Ibham *et al.* [29] examined the homogeneous charge compression ignition-direct ignition (HCCI-DI) engines using acetone, butanol, and ethanol blends. Acetone, butanol, and ethanol blends minimized NO_x emissions while enhancing BTHE and fuel economy. Christopher *et al.* [30] assessed the performance of biodiesel fuels produced from locally sourced canola and sunflower oil feedstocks in South Africa. They claimed that while nitrogen oxide emissions were higher with biodiesel and its diesel blends, smoke emissions were lower.

Based on extensive literature, EGR has emerged as a well-established technique for reducing NO_x emissions in compression ignition (CI) engines. This method involves recirculating exhaust gases, effectively diluting the intake air and lowering the combustion temperature, decreasing NO_x emissions. However, some research has been examined thus far on applying hybrid alternative biodiesel (specifically, no study has been conducted on a blend of 20% rubber seed oil and 80% waste plastic oil) at an optimized compression ratio of 20:1 in combination with EGR. To address this research gap, a recent experimental investigation employed a novel approach that involved variable EGR rates (0%, 5%, 10%, and 15% based on volume) with the hybrid alternative biodiesel while

maintaining a constant compression ratio. The foremost objective was to examine the special effects of EGR on combustion, performance characteristics, and emissions. These findings were then compared with those of standard diesel fuel and plain waste plastic oil to evaluate the potential benefits and drawbacks of the EGR strategy when combined with the hybrid alternative biodiesel.

MATERIALS AND METHODS

Production of rubber seed oil's methyl ester

Jatropha curcas, *Madhuca indica*, *Pongamia pinnata*, Rubber seed oil, etc., are examples of non-edible vegetable oils. Rubber seed is the cheapest and most widely available. India, an agricultural nation, is essential to producing rubber seed. A rubber tree may grow to a height of 25 to 35 meters. In India, 2.5 lakh hectares of rubber plantations generate 35,000 metric tons of seeds and 5,400 metric tons of raw oil annually from those seeds [20].

Figure 1a shows the representation of the rubber seed oil transesterification process. It has two esterification processes: acid esterification and alkaline esterification. This transesterification process can reduce free fatty acids from 22% to 2% while also lowering viscosity. After the transesterification procedure, rubber seed oil's methyl esters were produced.

Production of WPO

Nowadays, plastic materials are widely used, and the disposal of plastic waste is a serious problem. There are different methods of disposing of plastic waste, such as land filling, incineration, pyrolysis, and recycling. The most significant waste plastics are strapping, cable sheathing, plastic film, crates, pipes, and waste plastic from bottles, pots, tubs, and trays.

Waste plastics may be recycled in two different ways. They are recycling processes that use heat and catalysts to break down waste plastic. Thermal degradation is a simple method, whereas catalytic degradation uses the correct proportion of catalyst to plastic waste to yield the maximum amount of liquid hydrocarbon. In the current study, the thermal pyrolysis degradation of solid waste plastics is carried out in the absence of air at temperatures ranging from approximately 500 °C to 800 °C. Pyrolysis yields char and bio-oil. Temperature and heating rate are the key factors affecting how much bio-oil is generated during pyrolysis.

The pyrolysis plant's schematic design is shown in Figure S1 (Supplementary material). The pyrolysis

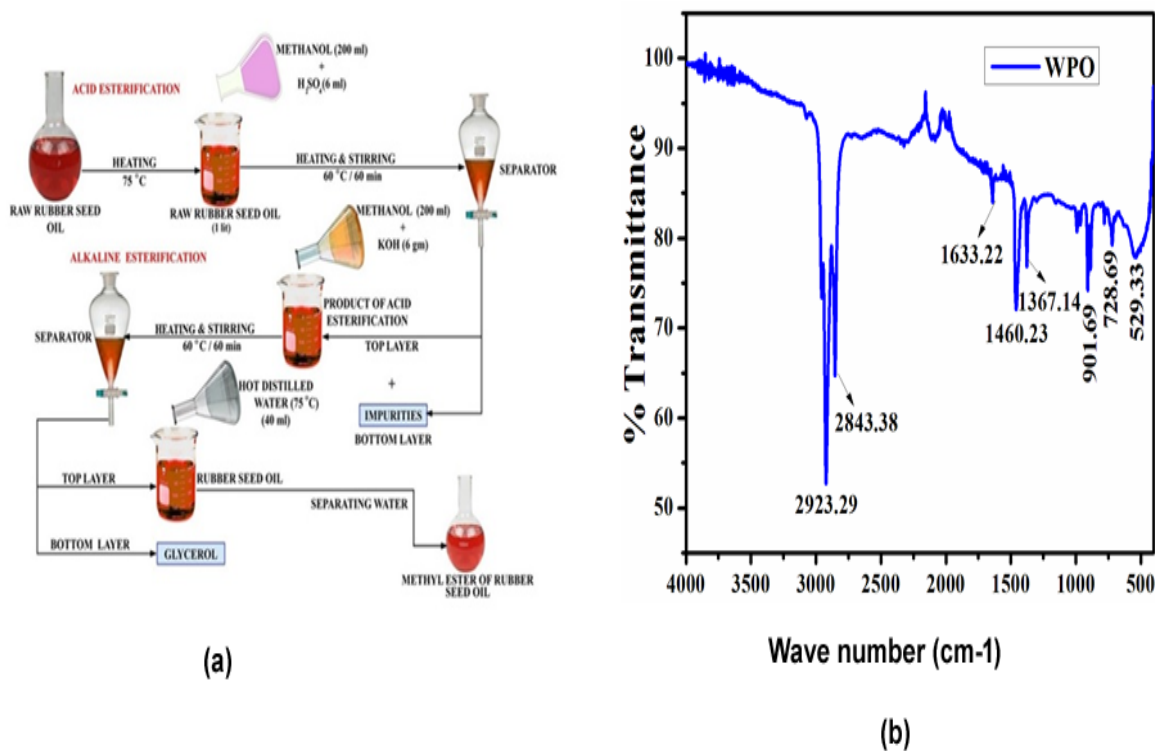


Figure 1. Diagram of (a) RSO esterification process (b) FTIR analysis of WPO.

plant consists of a reactor and a condenser unit. A thin sheet encloses the stainless-steel reactor, which has a diameter of 1300 mm. Three 1500-watt electrical heater coils are fixed to the reactor. Glass wool acts as an insulator and is placed between the reactor and the thin sheet. The reactor consists of a mechanical stirrer with motor, safety valve, pressure gauge, feed hopper with control valve, K-type thermocouple, hand hole, and control panel. The purpose of the stirrer is to ensure thorough mixing of the mixture and to uphold a temperature range of 500°C to 700°C within the reactor. The excess pressure is released through the safety valve. The reactor's temperature is measured by the thermocouple, displayed in the indicator on the control panel, and controlled by the controller. Following the pyrolysis process, approximately 20 to 25 percent of the waste is removed via a hand hole with a stopcock through the reactor's bottom. The reactor outlet is fixed to the condenser, which consists of a water container and cooling coil through which plastic vapor is condensed. The cooling coil is made up of a stainless-steel tube with a 20 mm diameter and 1800 mm length and is kept inside the water container with a 300 mm diameter and 500 mm height. The container has inlet and outlet valves through which water is circulated.

The condensed liquid is collected in a fuel collection tank made of stainless steel, and the time for delivery of the liquid fuel is around 3.5 hours after the

start of the pyrolysis process. The uncondensed gas is passed through an AVL 444 DiGas analyzer, then through a flame arrester containing water to prevent the backfire. Then, washed, uncondensed gas flows through the burner to produce a blue flame that reduces the pollutant in the atmosphere. The condensed liquid from the pyrolysis plant is fractionated using a distillation unit to produce WPO.

Fourier transform infrared spectroscopy (FTIR) analysis of waste plastic oil

The Agilent Cary 630 FTIR spectrometer with an ATR (Attenuated Total Reflectance) detector was used to find all the functional groups in waste plastic oil. The spectral range was from 4000 cm^{-1} to 500 cm^{-1} , with the highest resolution of 2 cm^{-1} . The findings of the WPO's FTIR investigation are shown in Figure 1b. The location of different bond vibrations, such as stretching, distortion, and bending, is described by many distinct peaks.

Table 1 lists the portion of the WPO spectrum that is distinctive. It can be seen from the FTIR spectra that the waste plastic oil has a peak at 2923.29 cm^{-1} , which corresponds to the stretching of hydrogen bonds and the stretching vibration of O-H bonds. Different peaks may be found in the FTIR spectra of WPO, ranging from 1633.22 to 529.33 cm^{-1} . Due to its strong bonding structure with rubber seed oil, the phenolic bond of WPO is the most significant one. There is no phase

Table 1. Characteristic region of WPO spectra.

WPO wave number	Chemical bond	Functional groups	Mode of vibration
529.33	Alkyl halides	C-Br	Stretch
728.69	Alkanes, Aromatics, Alkyl halides	CH ₂ , C-H, C-Cl	Bend, Bend (mono), Stretch
901.69	Alkenes, and anhydrides	C-H, C-O	Bend (monosubstituted), Stretch
1367.14	Alkanes, alkenes, ethers, ketones, alcohols and phenols	CH ₃ , C-O-C, C-C, O-H, C-H,	Bend, Bend in plane, Stretch (dialkyl), Stretch
1460.23	Alkanes and aromatics	CH ₂ , C=C	Bend, Stretch
1633.22	Alkenes, acids, and amides	C=C, C=O	Stretch (isolated & conjugated)
2843.38	Alkanes, aldehydes, and benzoic acid	C-H, O-H	Stretch, Aldehyde stretch
2923.29	Alkanes, benzoic acid, alcohols and phenols	C-H, O-H	Stretch

separation between these two oils when mixing.

Physiochemical properties of diesel, RSO, and WPO

The unique and important properties of biodiesel are cetane number, heating value, viscosity, etc. The viscosity of the biodiesel is a significant property because it influences the vaporization and atomization of the biodiesel. Compared to diesel, it is more lubricating and has higher cetane values. It helps in complete combustion, which increases the engine's energy output. The characteristics of biodiesel also contribute to less fuel system wear and longer fuel injector equipment life. The liquid biodiesel can range in color from golden to dark brown and has a high boiling point but little vapor pressure. Biodiesel has a density of 860 kg/m³, which is less than water's density, and a flash and fire point that is significantly greater than that of diesel. It has a lower calorific value than diesel and almost no sulfur. Hence, it is used as an additive to diesel. Table 2 summarises the significant physiochemical characteristics of diesel, RSO, and WPO.

Table 2. Diesel, RSO, and WPO's physiological and chemical characteristics.

Properties	Diesel	RSOME	WPO	R-20/P-80
Specific gravity at 15 °C	0.82	0.8102	0.915 5	0.893
Net Calorific value, kJ/kg	44800	38650	43340	41362.4
Flash point, °C	50	66	54	56
Fire point, °C	57	68	56	58
Kinematic viscosity at 40 °C, cSt	2	12.75	3.18	3.704
Cetane index	50	56	51	38.4
Water content, wt. %	0.025	0.3	0.01	0.065
Oxygen by difference, %	Nil	22	1.5	5.6

Experimental setup

The EGR system, instrumentation, and experimental setup specifics employed in this study are provided. Figure 2 displays a photographic representation of the experimental setup. An engine with a rated output of 3.7 kW @ 1500 rpm and built on the Kirloskar platform was used in this inquiry. It was vertical, naturally aspirated, and water-cooled. The engine was loaded and unloaded using an eddy current dynamometer coupled to a strain gauge load cell. A Cityzen piezoelectric, air-cooled, durable pressure sensor with a built-in charge amplifier and 360° pulse crank angle encoder was included in this configuration to monitor the combustion pressure and associated crank angle. Data acquisition (DAS) systems were used to gather, store, and analyze data while conducting experiments, and they link pressure sensor inputs to computers.

The cooling water circulation to the engine and calorimeter was measured using rotameters—the computer's "Engine Test Express v14" software package analyzed combustion and engine performance. A burette with top and bottom optical sensors was used to assess fuel usage. The top sensor signals the DAS to begin the counter time as soon as fuel has flowed through it. When fuel reached the bottom sensor, it signaled the DAS to halt the timer and replenish the burette from the fuel tank. This process was repeated three times. It allowed for calculating the engine's mass fuel consumption at varied loads. The air mass consumed was determined using a differential pressure sensor installed in the air surge tank. A K-type thermocouple (AD595) installed in the exhaust manifold measured exhaust gas temperature. A non-contact proximity speed sensor of the PNP (positive negative positive) kind that was mounted close to the flywheel was used to measure the engine speed. Table 3 contains all of the test engine's data.

Exhaust gas recirculation system (EGR)

EGR is one of the best and most often used methods for lowering the output of NO_x from internal

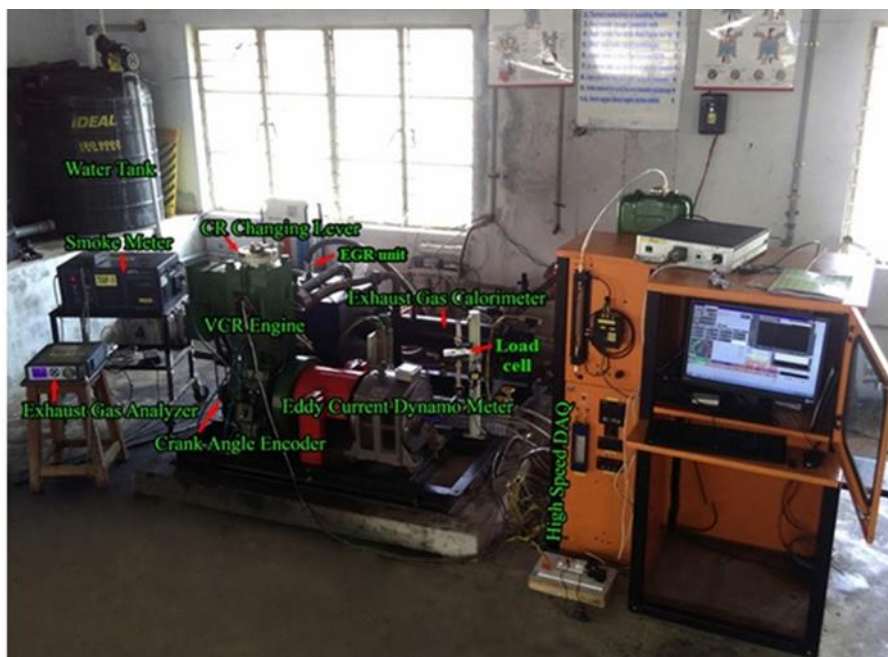


Figure 2. Photo view of experimental set-up.

Table 3. Technical details of the experiment's configuration.

Particulars	Specifications
Make and Model	Variable compression ratio multi-fuel, vertical, water-cooled, direct injection, naturally aspirated engine. Legion Brothers, Bangalore, modified the engine to change the compression ratio arrangement. The Kirloskar AV1 engine makes the base crankcase.
Compression ratio range	6:1 to 20:1
Rated brake power	3.7 kW
Rated speed	1500 rpm
No. of cylinders / No. of strokes	01 / 04
Bore x Stroke	80 x 110 mm
Displacement volume	552.64 cc
Nozzle opening pressure	200 bar
Maximum load	10 kg
Speed measurement	PNP-type non-contact proximity speed sensor
Fuel flow measurement	Make - HONEYWELL; Model - LLE102000.
Airflow measurement	Make - Silicon Microstructure Incorporated; Model - SM5812/SM5852
Software	"Engine Test Express v14" Engine performance analysis software

combustion engines. EGR comes in two different varieties: cooled and uncooled. The former is efficient because cooled exhaust gas is mixed with fresh air in the air surge tank, which reduces the temperature and oxygen proportion necessary for combustion.

The EGR maximizes the specific heat of the input charge due to mixing, which results in minimum flame temperatures for a given combustion chamber heat release. This mixture's entrance into the engine cylinder lowers the maximum temperature in the combustor, which lowers the generation of NO_x. The cooled dissipative gas temperature was maintained

below the atmospheric temperature by varying the circulation rate of cold water circulated through the EGR unit. The cooled exhaust gas was passed through a fabric filter before entering the surge tank because the surge tank had particulate matter and soot, which affected the burning phenomenon. The exhaust gas was taken through an orifice in the manifold and sent to the gas regulator system to regulate the recirculation quantity. Generally, the range of EGR was about 5% to 20% of exhaust gas.

Utilizing a differential pressure sensor, the flow rate of EGR was calculated by measuring the EGR

volume in millimeters of water column. The volume of EGR in the air surge tank divided by the total charge introduced into the cylinder was used to compute the EGR percentage (Sum of engine air intake and EGR volume in millimeters of water column). EGR% equals [volume of EGR/total charge injected into the cylinder] * 100. The benefits of EGR are as follows: EGR can be used in engines without affecting efficiency or fuel economy. It also reduces NO_x emissions. The EGR unit is shown in Figure S2.

Experimental errors and uncertainties

The measuring instruments used in the tests were standardized, and the error rates for each were calculated to lower the measurement error rate to the lowest percentage achievable.

Total percent of uncertainty = $\sqrt{\{ \text{uncertainty of } [(TFC)^2 + (\text{load})^2 + (\text{BTHE})^2 + (\text{CO})^2 + (\text{HC})^2 + (\text{NO}_x)^2 + (\text{SO})^2 + (\text{EGT})^2 + (\text{pressure pickup})^2] \}} = \sqrt{\{ (1)^2 + (0.2)^2 + (1)^2 + (0.2)^2 + (0.2)^2 + (0.2)^2 + (1)^2 + (0.15)^2 + (1)^2 \}} = \pm 2.28 \%$.

RESULTS AND DISCUSSION

Six experiments were conducted to evaluate performance factors, such as BTHE and BSFC emissions, including NO_x, CO, UBHC, smoke, and EGT. These experiments involved varying the fuel and EGR conditions. The initial test exclusively employed diesel fuel, the second utilized WPO exclusively, and

the other four employed hybrid biodiesel. The hybrid biodiesel experiments were conducted under different EGR conditions: without EGR, with 5% EGR, 10% EGR, and 15% cooled EGR. All tests were conducted on a compression ignition engine with an optimum compression ratio of 20:1.

Diagram of a pressure-crank angle

Figure 3a illustrates the variations in cylinder pressure patterns under different load conditions for various fuel types and EGR percentages. At full load, diesel exhibits a peak pressure of 62 bar, while hybrid biodiesel without EGR reaches a peak pressure of 70 bar. For hybrid biodiesel with 5%, 10%, and 15% EGR at full load, the peak pressures are 69.1 bar, 68.54 bar, and 68.4 bar, respectively. The maximum pressure for WPO without EGR and at full load is 67 bar.

The decrease in combustion chamber pressure can be observed as the EGR percentage increases. When the EGR circulation rate increases from 0% to 5%, peak pressure readings are lower by 1.28%. Similarly, as the EGR circulation rate rises from 5% to 10%, peak pressure values decrease by around 0.81%. Additionally, as the EGR circulation rate rises from 10% to 15%, peak pressure values decrease by around 0.2%. In the case of hybrid biodiesel with 15% EGR, the peak pressure is approximately 2.28% lower than it would be without EGR. The fundamental cause is that introducing these exhaust gases absorbs the heat energy released during combustion, thereby reducing the cylinder pressure [17].

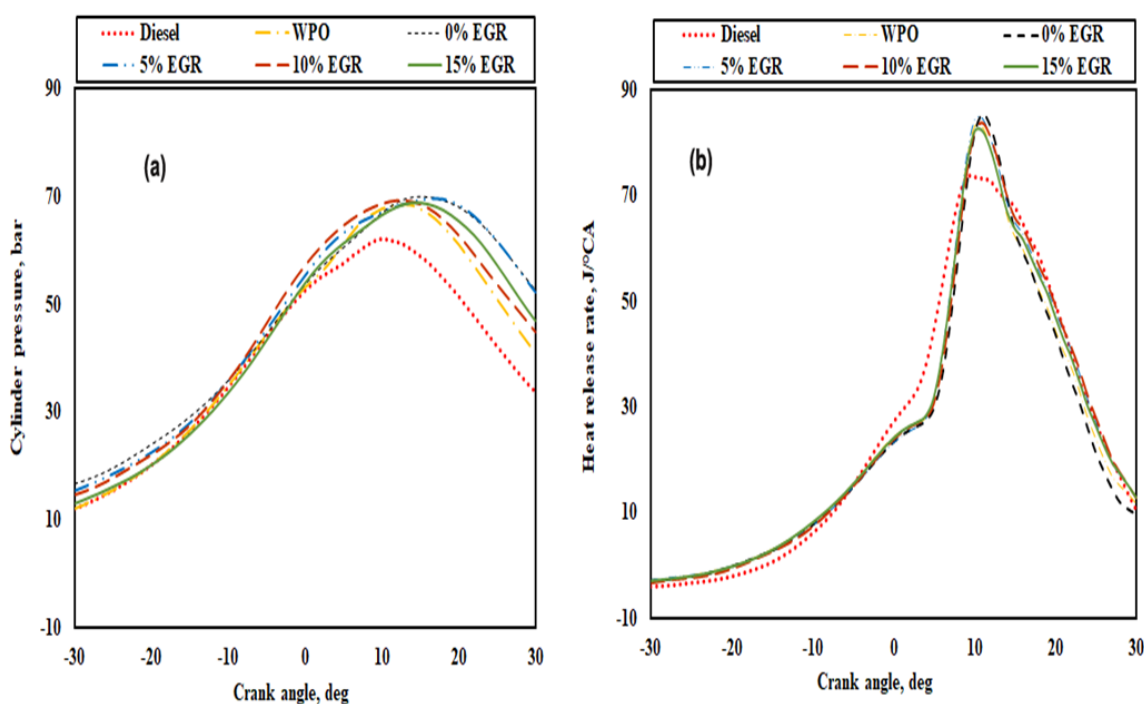


Figure 3. Variation of engine parameters at full load conditions (a) Pressure versus crank angle (b) HRR versus crank angle.

Rate of heat releas

Figure 3b depicts the variation in the heat release rate for the studied fuels at different EGR percentages under typical operating conditions at full load and various crank angles. The heat energy potential in the heat release rate curve is transformed into useful work. In correlation with the increase in EGR levels, Figure 3(b) illustrates a decline in the maximum heat release rate. Under typical operating conditions, diesel and WPO exhibit maximum heat release rates of $73 \text{ J/}^\circ\text{CA}$ and $83 \text{ J/}^\circ\text{CA}$, respectively. However, its value decreases for hybrid fuel at full load from $85.38 \text{ J/}^\circ\text{CA}$ without EGR to $82.28 \text{ J/}^\circ\text{CA}$ with 15% EGR. Additionally, it is noteworthy that for hybrid biodiesel at 100% load, the peak rate of heat release values are $84.61 \text{ J/}^\circ\text{CA}$ and $83.79 \text{ J/}^\circ\text{CA}$ for 5% and 10% EGR, respectively. As the EGR circulation rate rises from 0% to 15%, the reduction in heat release rate values is around 3.63%. Conversely, as the EGR circulation rate rises from 5% to 10%, the reduction in heat release rate values is around 0.96%. The drop-in heat release rate is attributed to the drop in oxygen concentration, accompanied by a rise in EGR level and a shorter ignition delay. The primary factor contributing to the reduction in NO_x emissions is the decrease in heat release rate, which leads to a decrease in peak combustion temperature [19]. The hybrid biodiesel exhibits higher heat emission capacity without EGR operation owing to the availability of excess oxygen for the combustion process.

Ignition delay

The delay period, commonly called ignition delay, denotes the period or crank position stuck between the initiation of injection and the onset of ignition. Ignition delay can be divided into two components: physical and chemical. For fuel to be atomized, mixed, and vaporized, there must be a physical delay. Chemical delay encompasses pre-combustion reactions that impact the thermodynamic efficiency and pre-combustion mixture of air and fuel vapor. Several factors influence the delay period, including injection pressure, nozzle orifice size and design, cylinder air pressure and temperature, fuel viscosity, droplet size distribution, droplet velocities, and fuel volatility. The delay time impacts in-cylinder pressure, NO_x emissions, the combustion phase, and the heat release rate. Under normal operating conditions, the ignition delays of hybrid biodiesel are compared across different EGR percentages and load conditions for all investigated oils, as shown in Figure 4a. Without EGR and at full load, the ignition delays for diesel and hybrid biodiesel are $10.8 \text{ }^\circ\text{CA}$ and $10.5 \text{ }^\circ\text{CA}$, respectively. The ignition delays for hybrid biodiesel with 5, 10, and 15% EGR at full load are $10.3 \text{ }^\circ\text{CA}$, $10.21 \text{ }^\circ\text{CA}$, and

$10.11 \text{ }^\circ\text{CA}$, respectively. WPO exhibits an ignition delay of $11.8 \text{ }^\circ\text{CA}$ at full load without EGR.

With the rise in the EGR circulation rate from 0–5%, there is a 1.9% reduction in ignition delay values. Similarly, when the EGR circulation rate rises from 10–15%, the reduction in ignition delay values is around 0.98%. It can be observed that all ignition delays for hybrid biodiesel tend to decrease as the load and EGR increase. It is primarily due to higher internal temperatures at increased loads, which decrease chemical delay and consequently shorten the ignition delay period. Additionally, as the EGR percentage rises, the inlet air temperature increases due to EGR, contributing to a slight decrease in ignition delay [23].

Cylinder peak pressure

Figure 4b shows the results of the study, which looked at how the maximum cylinder pressure changed with load for different fuels with and without EGR. The figure demonstrates that the highest pressure in the cylinder increases with increasing load and decreases with higher EGR flow rates. The amount of fuel delivered, the petroleum fuel volatility, and the ignition delay duration are the key factors determining the maximum cylinder pressure. At full load, the relative peak pressures in the diesel and hybrid biodiesel cylinder are 62 bar, 70 bar, 69.1 bar, 68.54 bar, and 68.4 bar at 0%, 5%, 10%, and 15% EGR, respectively. WPO's maximum cylinder pressure at full load without EGR is 67 bar. When the EGR circulation rate rises from 0% to 5%, the reduction in cylinder peak pressure is around 1.28%. Similarly, when the EGR circulation rate rises from 10% to 15%, the reduction in cylinder peak pressure values is around 0.2%. It is noted that the decrease in maximum cylinder pressure is more significant from 0% to 15% EGR rates due to the reduction in oxygen within the engine cylinder [19].

Brake thermal efficiency (BTHE)

The variation in braking thermal performance for the studied fuels at different EGR rates under varying loads is depicted in Figure 4c. For diesel, WPO, and hybrid biodiesel without EGR operation, the BTHEs are 26.8%, 23.4%, and 30.5%, respectively, at full capacity. When the vehicle is fully loaded, the BTHE is 31% with 5% EGR, 31.8% with 10% EGR, and 31.5% with 15% EGR. When the EGR circulation rate rises from 0–5%, the increase in BTHE is around 1.63%. Similarly, when the EGR circulation rate rises from 5–10%, the increase in BTHE is around 2.58%. The return of exhaust gas to the engine leads to an elevation in the temperature of the intake charge, a faster combustion velocity, and the mixing of dissipated gases with fresh air, resulting in improved fuel combustion.

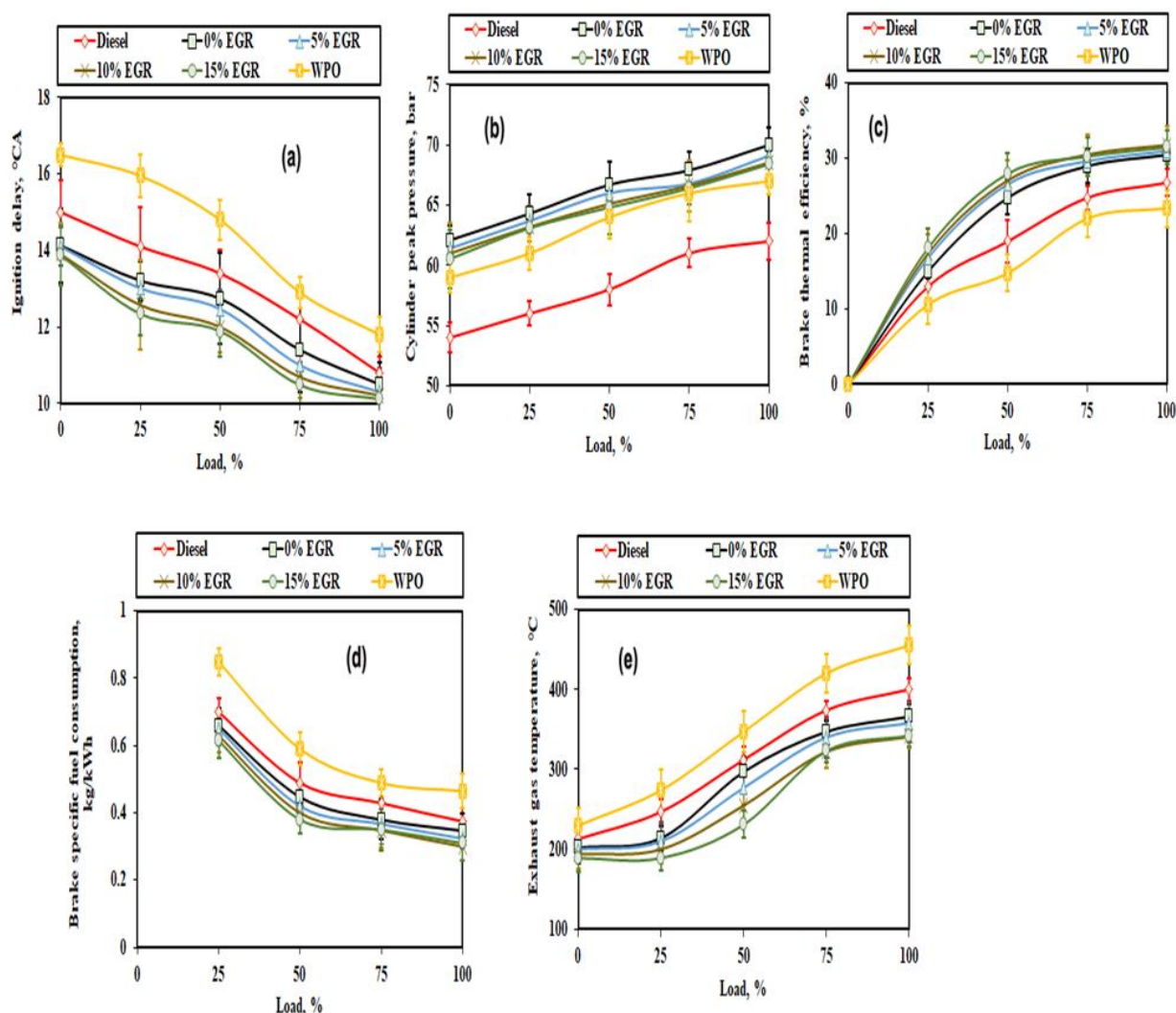


Figure 4. Variation of engine parameters at different load conditions: (a) Ignition delay; (b) Cylinder peak pressure; (c) Brake thermal efficiency (d) Brake specific fuel consumption; (e) Exhaust gas temperature.

Consequently, the thermal efficiency of the engine experiences a marginal increase. A contrasting observation occurs when the EGR circulation rate rises from 10 to 15%. In this scenario, there is a slight decrease of approximately 0.94% in BTHE values. The presence of CO₂ and unburned hydrocarbons in the exhaust gas can potentially reduce oxygen availability in the combustion chamber, causing a decline in BTHE values for the diesel engine [24]. It is important to note that the optimal EGR rate for achieving the highest thermal efficiency may vary depending on specific engine design, fuel type, and operating conditions. Excessive dilution from excessively high EGR rates can negatively impact combustion and overall thermal efficiency.

Brake specific fuel consumption (BSFC)

Figure 4d illustrates the deviation in BSFC for the investigated fuels under varied loads and EGR rates. At

0% EGR and full load, the BSFC values for WPO and diesel are 0.465 and 0.375 kg/kWh, respectively. While the vehicle is fully loaded, the BSFC values for hybrid biodiesel blends are 0.347, 0.324, 0.3, and 0.31 kg/kWh for 0, 5, 10, and 15% EGR, respectively. With a rise in the EGR circulation rate from 0–5%, there is a slight decrease of approximately 6.63% in BSFC values. Similarly, with a rise in the EGR circulation rate from 5 to 10%, there is a 7.4% decrease in BSFC. BSFC decreases up to 10% of the EGR rate. The recirculated exhaust gases contribute energy to the fresh air and fuel mix during burning, reducing the amount of hybrid biodiesel consumed. As a result, fuel consumption related to braking is reduced. However, with an increase in the EGR circulation rate from 10–15%, there is a slight increase of approximately 3.33% in BSFC values. It increases in BSFC at a 15% EGR rate and at 75% and 100% load, which can be attributed to forming a rich mixture and reducing in-cylinder temperatures, leading to incomplete combustion [25].

Exhaust gas temperature

Figure 4e showcases the variations in EGT for the studied fuels under varied loads and EGRs. As can be seen, at full load, the exhaust temperatures for waste plastic oil and diesel are 455 °C and 400 °C, respectively, while the EGT for hybrid biodiesel without EGR is 366 °C. For hybrid biodiesel at full load with 5% EGR, the exhaust gas temperature is 358 °C; with 10% and 15% EGR, it decreases to 341 °C and 342 °C, respectively. When the EGR circulation rate rises from 0–5%, there is a slight decrease of approximately 2.18% in EGT values. Similarly, with a rise in the EGR circulation rate from 5–10%, the reduction in EGT is around 4.74%. The peak combustion temperature decreases as the EGR increases. It indicates a more efficient heat energy utilization with a shorter ignition delay. As a result, the exhaust gas temperature decreases, leading to a reduction in NO_x emissions. Increased mixing duration, prolonged burn dilution, a higher heat capacity mixture, and separation from the more complex EGR molecules contribute to the lowered flame temperatures and subsequent decrease in EGT [20].

Oxides of nitrogen emissions

Most NO_x emissions consist of nitrogen dioxide and nitric oxide, and their levels are influenced by temperature, oxygen content, and reaction rate. Figure 5a illustrates the significant reduction in NO_x

emissions achieved by implementing EGR for the studied fuels. Observed NO_x emissions for WPO, diesel, and hybrid biodiesel at full load are 1010 ppm, 820 ppm, and 1095 ppm, respectively, without EGR activation. At full load, hybrid biodiesel NO_x emission values are 1059 ppm, 900 ppm, and 800 ppm, respectively, for 5%, 10%, and 15% EGR.

With a rise in the EGR circulation rate from 0–5%, there is a 3.28% decrease in NO_x emissions. Similarly, as the EGR circulation rate rises from 5% to 10%, the reduction in NO_x is around 15%. Additionally, with a rise in the EGR circulation rate from 10% to 15%, there is an 11.11% decrease in NO_x emissions. The primary factors contributing to the decrease in NO_x emissions with increasing EGR percentages are the increase in total working gas heat capacity and the decrease in combustion temperature. It might be because the exhaust fumes contain inert gases like carbon dioxide and water vapor. When these exhaust gases are recirculated and blended with the intake air, the ancillary gases absorb the heat energy generated during burning, lowering the combustion temperature. Moreover, the EGR substitutes air for O₂ in the combustible chamber, lowering the combustion temperature. At higher EGR rates, NO_x emissions can be significantly reduced. On the other hand, higher EGR rates result in higher emissions of HC, CO, and smoke opacity [26].

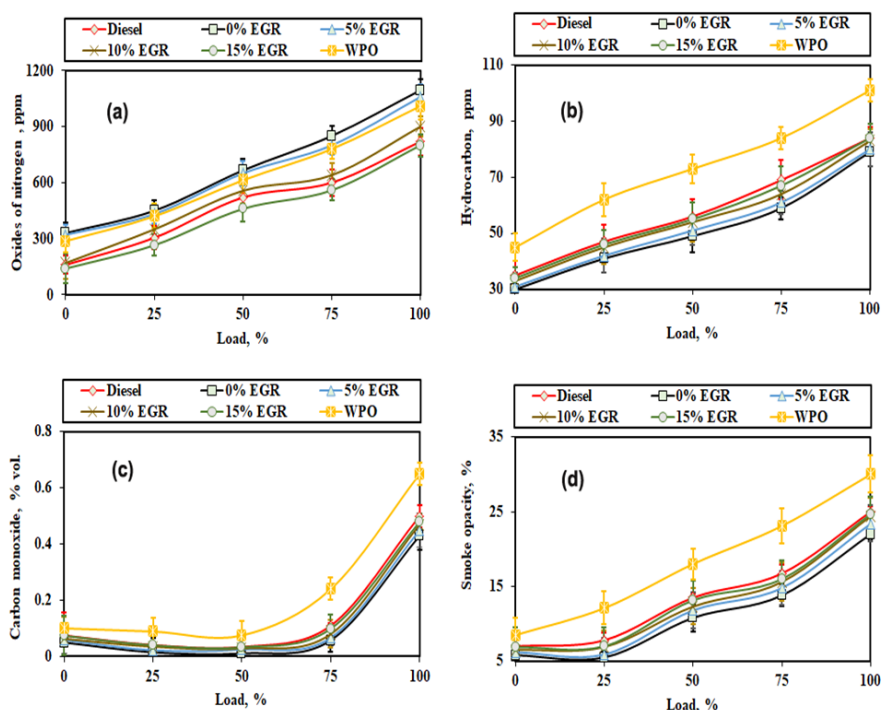


Figure 5. Variation of emissions with different load conditions: (a) Oxides of nitrogen; (b) Hydrocarbon; (c) Carbon monoxide; (d) Smoke opacity.

Hydrocarbon emissions

Figure 5b shows the hydrocarbon (HC) emissions from the variable compression ratio engine for the tested fuels under different loads and EGR rates. Without EGR and at full load, neat WPO exhibits HC emission levels of 101 ppm. Additionally, hybrid biodiesel and diesel display HC emissions of 79 ppm and 84 ppm at full load without EGR, respectively. Under full load, hybrid biodiesel yields HC concentrations of 80 ppm, 83 ppm, and 84 ppm with 5%, 10%, and 15% EGR, respectively. When the EGR circulation rate rises from 0–5%, the increase in HC emissions is around 1.26%. Similarly, with an increase in the EGR circulation rate from 5–10%, there is a slight increase of approximately 3.75% in HC emissions. Furthermore, when the EGR circulation rate rises from 10–15%, the increase in HC emissions is around 1.2%. These increases in HC emissions can be attributed to the higher recirculation of exhaust gases through the engine, which reduces the amount of oxygen available in the combustion chamber. Consequently, more hydrocarbon emissions are produced. Additionally, incomplete combustion occurs due to a lower oxidation rate in the chamber, further contributing to the elevated levels of hydrocarbon emissions in the exhaust gases [26].

Carbon monoxide emissions

During the burning of hydrocarbon fuels, carbon monoxide (CO) is produced as an intermediate by-product, and incomplete combustion leads to CO emissions. Figure 5c illustrates the variations in CO emissions with different loads and EGR rates for the tested fuels. At full load without EGR operation, the CO levels for hybrid biodiesel, diesel, and waste plastic oil (WPO) were found to be 0.43% volume, 0.5% volume, and 0.65% vol., respectively. For 5%, 10%, and 15% EGR operations at full load, the CO emissions are 0.45% volume, 0.47% volume, and 0.48% vol., respectively. With an increase in the EGR circulation rate from 0–5%, there is a slight increase in CO emissions, approximately 4.65%. Similarly, with an increase in the EGR circulation rate from 5 to 10%, the increase in CO emissions is around 4.44%. Furthermore, when the EGR circulation rate rises from 10–15%, the increase in CO emissions is around 2.12%. It is evident that as the EGR level rises, so do the CO emissions. Insufficient oxygen in the intake air leads to incomplete combustion, the primary cause of increased CO emissions. This incomplete combustion is responsible for the higher CO emissions observed at full load. However, lower EGR percentages result in significantly lower CO emissions. With higher EGR percentages, there is a slight rise in CO emissions owing to the insufficient burning of hybrid biodiesel

caused by oxygen deficiency. However, the additional oxygen concentration in the biodiesels compensates for the lack of oxygen during EGR operation [26]. As a result, the hybrid biodiesel emits less CO than diesel and WPO at all EGR levels.

Smoke opacity emissions

Figure 5d displays the smoke opacity variations with different loads and EGR rates for hybrid biodiesel, diesel, and WPO. At full load without EGR, the smoke opacity emissions for diesel and WPO are 25% and 30%, respectively, while they are 22% for hybrid biodiesel. Similarly, with 5%, 10%, and 15% EGR at full load, the observed smoke opacity emissions are 23.4%, 24.41%, and 24.7%, respectively. When the EGR circulation rate rises from 0–5%, the increase in smoke opacity is around 6.36%. Likewise, with an increase in the EGR circulation rate from 5 to 10%, there is a slight increase in smoke opacity, approximately 4.31%. Furthermore, when the EGR circulation rate rises from 10–15%, the increase in smoke opacity is around 1.18%. As the EGR percentages rise, the emissions' smoke opacity also rises. The increase in smoke opacity emission is insignificant initially and considerably increases, particularly at higher loads with EGR, because of the partial oxygen replenishment caused by the recirculation of exhaust gases. Also, this demonstrates a decrease in smoke opacity emissions from hybrid biodiesel compared to diesel at all loads [21].

Table 4 compares hybrid biodiesel with different EGRs to diesel at full load, expressed as a percentage increase or decrease.

CONCLUSION

Based on the comprehensive investigation, the following key findings were identified. The utilization of a 10% EGR rate with hybrid biodiesel resulted in improved combustion, performance, and emissions in the VCR engine compared to other test conditions. The utilization of 15% EGR led to a 4% decrease in peak pressure for hybrid biodiesel, highlighting the impact of EGR on combustion dynamics. At fully loaded conditions and with a CR of 20:1, the BTHE for the hybrid biodiesel reached the maximum level of 31.8% when employing 10% EGR. The implementation of hybrid alternative diesel fuel in a compression ignition engine, along with a compression ratio of 20:1 and 10% EGR, resulted in notable outcomes. These include a low exhaust gas temperature of 341°C and minimal fuel consumption, as represented by the BSFC value. Elevated EGR levels slightly increased hydrocarbon, carbon monoxide, and smoke opacity emissions due to

Table 4. A comparison of hybrid biodiesel with different EGR to diesel at full load.

Sl. No.	Parameter	0% EGR	5% EGR	10% EGR	15% EGR
Combustion Parameters					
1	Ignition delay (°CA)	-2.78	-4.63	-5.46	-6.39
2	Maximum heat release (J/°CA)	+16.96	+15.9	+14.78	+12.71
3	Maximum cylinder pressure (bar)	+12.9	+11.45	+10.55	+10.32
Performance parameters					
1	Brake thermal efficiency (%)	+13.81	+15.67	+18.66	+17.54
2	Brake-specific fuel consumption (kg/kWh)	-7.47	-13.6	-20	-17.33
3	Exhaust gas temperature (°C)	-8.5	-10.5	-14.75	-14.5
Emission parameters					
1	Oxides of nitrogen emission (ppm)	+33.54	+29.15	+9.76	-2.43
2	Hydrocarbon emission (ppm)	-5.95	-4.76	-1.19	0
3	Carbon monoxide emission (% volume)	-14	-10	-6	-4
4	Smoke opacity emission (%)	-12	-6.4	-2.36	-1.2

“+” indicates percentage increase; “-” indicates percentage decrease.

reduced fresh air flow into the VCR engine. However, it has reduced ignition delay in the cylinder and lowered NO_x emissions in all tests. These findings highlight the potential advantages and applications of hybrid fuel in diverse sectors such as automotive, power generation, maritime applications, etc.

FUTURE SCOPE

For the exploration of the use of mixtures of rubber seed oil and waste plastic oil as fuel in variable compression ratio engines driven by EGR, the following future works are advised. Especially low-speed heavy-duty engines (diesel power generators) and multi-cylinder diesel engines (Heavy vehicles) should be tested for the RSO-WPO mixtures. Diesel engines with minimal heat rejection should be tested for alternative fuel alone (waste plastic oil and rubber seed oil). A numerical study on the effect of EGR on emissions and performance characteristics of a compression ignition engine using hybrid and alternative fuel. To enhance the quality of the WPO and improve its combustion properties, a novel process can be implemented to remove water and oxygen content, thereby reducing the risk of engine component rust and increasing the fuel's calorific value. In future research, parameters like injection diameter, fuel mass, and surface tension will be considered when analyzing EGR's variable compression ratio engine.

NOMENCLATURE

R-20/P-80	20% RSO blended with 80% WPO
A/F	Air fuel ratio

ARAI	Automotive Research Association of India
BSO	Babassu oil
bTDC	Before top dead centre, °CA
BP	Brake power, kW
BSFC	Brake specific fuel consumption, kg/kWh
BTHE	Brake thermal efficiency, %
CO	Carbon monoxide, % volume
cSt	Centi Stoke
DAS	Data acquisition system
EGT	Exhaust gas temperature, °C
HC	Hydrocarbon, ppm
JME	Methyl ester of <i>Jatropha curcas</i>
KME	Methyl ester of Karanja oil
MSW	Municipal Solid Waste
NO	Nitric Oxide
NO ₂	Nitrogen Dioxide
NO _x	Oxides of nitrogen, ppm
KOH	Potassium hydroxide
SFC	Specific fuel consumption, kg/kWh
H ₂ SO ₄	Sulfuric acid
VCR	Variable compression ratio
EGR	Exhaust gas recirculation
WPO	Waste plastic oil

REFERENCES

- [1] M.S.N. Awang, N.W. Mohd Zulkifli, M.M. Abbas, S. Amzar Zulkifli, M.A. Kalam, M.H. Ahmad, W.M.A.W. Daud, ACS

- Omega 6(33) (2021) 21655–21675.
<https://doi.org/10.1021/acsomega.1c03073>.
- [2] C. Kaewbuddee, E. Sukjit, J. Srisertpol, S. Maithomklang, K. Wathakit, N. Klinkaew, W. Arjharn, *Energies* 13(11) (2020) 2823. <https://doi.org/10.3390/en13112823>.
- [3] R.D. Arjanggih, J. Kandedo, *J. Energy Inst.* 93(3) (2020) 934–952. <https://doi.org/10.1016/j.joei.2019.08.005>.
- [4] D. Damodharan, B. Rajesh Kumar, K. Gopal, M.V. De Pours, B. Sethuramasamyraja, *Rev. Environ. Sci. Bio/Technol.* 18(4) (2019) 681–697.
<https://doi.org/10.1007/s11157-019-09516-x>.
- [5] S. Kumar, R. Prakash, S. Murugan, R.K. Singh, *Energy Convers. Manage.* 74 (2013) 323–331.
<https://doi.org/10.1016/j.enconman.2013.05.028>.
- [6] M. Mani, G. Nagarajan, S. Sampath, *Energy* 36 (2011) 212–219. <https://doi.org/10.1016/j.energy.2010.10.049>.
- [7] A.N. Ozsezen, M. Canakci, Ali Turkcan, C. Sayin, *Fuel* 88 (2009) 629–636.
<https://doi.org/10.1016/j.fuel.2008.09.023>.
- [8] Y.H. Chen, T.H. Chiang, J. H. Chen, *Fuel* 92 (2012) 377–380. <https://doi.org/10.1016/j.fuel.2011.08.018>.
- [9] P.K. Devan, N.V. Mahalakshmi, *Appl. Energy* 86 (2009) 675–680. <https://doi.org/10.1016/j.apenergy.2008.07.008>.
- [10] S.M. Ashrafur Rahman, H.H. Masjuki, M.A. Kalam, M.J. Abedin, A. Sanjid, H. Sajjad, *Energy Convers. Manage.* 76 (2013) 362–367.
<https://doi.org/10.1016/j.enconman.2013.07.061>.
- [11] N. Usta, E. Ozturk, O. Can, E.S. Conkur, S. Nas, A.H. Con, A.C. Can, M. Topcu, *Energy Convers. Manage.* 46 (2005) 741–755.
<https://doi.org/10.1016/j.enconman.2004.05.001>.
- [12] M. Habibullah, I.M. Rizwanul Fattah, H.H. Masjuki, M.A. Kalam, *Am. Chem. Soc.* 29(2) (2015) 734–743.
<https://doi.org/10.1021/ef502495n>.
- [13] S. Imtenan, H.H. Masjuki, M. Varman, M.A. Kalam, M.I. Arbab, H. Sajjad, S.M. Ashrafur Rahman, *Energy Convers. Manage.* 83 (2014) 149–158.
<https://doi.org/10.1016/j.enconman.2014.03.052>.
- [14] C.D. Rakopoulos, D.C. Rakopoulos, D.T. Hountalas, E.G. Giakoumis, E.C. Andritsakis, *Fuel* 87 (2008) 147–157.
<https://doi.org/10.1016/j.fuel.2007.04.011>.
- [15] H. Venu, L. Subramani, V. D. Raju, *Renew. Energy* 140 (2019) 245–263.
<https://doi.org/10.1016/j.renene.2019.03.078>.
- [16] M. Zheng, G.T. Reader, J.G. Hawley, *Energy Convers. Manage.* 45(6) (2004) 883–900.
[https://doi.org/10.1016/S0196-8904\(03\)00194-8](https://doi.org/10.1016/S0196-8904(03)00194-8).
- [17] O. Can, E. Ozturk, H. Solmaz, F. Aksoy, C. Cinar, H. Serdar Yucesu, *Appl. Therm. Eng.* 95 (2016) 115–124.
<https://doi.org/10.1016/j.applthermaleng.2015.11.056>.
- [18] V.J.J. Prasad, N. Hari Babu, B.V. Appa Rao, J. *Renewable Sustainable Energy* 1 (2009) 053104.
<https://doi.org/10.1063/1.3255043>.
- [19] M. Mani, G. Nagarajan, S. Sampath, *Fuel* 89 (2010) 1826–1832. <https://doi.org/10.1016/j.fuel.2009.11.009>.
- [20] A.S. Ramadhas, C. Muraleedharan, S. Jayaraj, *Clean* 36(12) (2008) 978–983.
<https://doi.org/10.1002/clean.200800108>.
- [21] A. Tsolakis, A. Megaritis, M.L. Wyszynski, K. Theinnoi, *Energy* 32 (2007) 2072–2080.
<https://doi.org/10.1016/j.energy.2007.05.016>.
- [22] K. Venkateswarlu, B.S.R. Murthy, V.V. Subbarao, K. Vijaya Kumar, *Front. Energy* 6(3) (2012) 304–310.
<https://doi.org/10.1007/s11708-012-0195-9>.
- [23] B. Rajesh kumar, S. Saravanan, *Fuel* 160 (2015) 217–226. <https://doi.org/10.1016/j.fuel.2015.07.089>.
- [24] K. Srinivasa Rao, *Int. J. Mech. Mechatron. Eng.* 16(2) (2016) 64–69.
<https://www.researchgate.net/publication/303573496>.
- [25] S. Park, H. Kim, B. Choi, *J. Mech. Sci. Technol.* 23 (2009) 2555–2564. <https://doi.org/10.1007/s12206-009-0704-x>.
- [26] H.E. Saleh, *Fuel* 88 (2009) 1357–1364.
<https://doi.org/10.1016/j.fuel.2009.01.023>.
- [27] M.B. Tasić, M.S. Stanković, M.D. Kostić, O.S. Stamenković, V.B. Veljković, *Chem. Ind. Chem. Eng. Q.* 28 (2022) 237–245.
<https://doi.org/10.2298/CICEQ210819035T>.
- [28] N.D.L.D. Silva, F.P.V. Loz, J.I. Soletti, D.D.G. Coelho, *Chem. Ind. Chem. Eng. Q.* 27 (2021) 155–163.
<https://doi.org/10.2298/CICEQ191117034S>.
- [29] I. Veza, A.T. Hoang, A.A. Yusuf, S.G. Herawan, M.E.M. Soudagar, O.D. Samuel, M.F.M. Said, A.S. Silitonga, *Fuel* 333 (2023) 126377.
<https://doi.org/10.1016/j.fuel.2022.126377>.
- [30] C. Enweremadu, O. Samuel, H. Rutto, *Environ. Clim. Technol.* 26(1) (2022) 630–647.
<https://doi.org/10.2478/rtuct-2022-0048>.

ANANTHAKUMAR
SUDALAIMANI¹
BARATHIRAJA RAJENDRAN²
THIYAGARAJ JOTHI³
ASHOKKUMAR
MOHANKUMAR⁴

¹Department of Mechanical
Engineering, Government
College of Engineering,
Tirunelveli, Tamil Nadu, India

²Department of Mechanical
Engineering, Einstein College of
Engineering, Near MS University,
Tirunelveli, Tamil Nadu, India

³Department of Mechatronics
Engineering, Er. Perumal
Manimekalai College of
Engineering, Hosur, Tamil Nadu,
India

⁴Department of Mechanical
Engineering, Government
College of Engineering, Bargur,
Krishnagiri, Tamil Nadu, India

EFEKTI RECIRKULACIJE IZDUVNIH GASOVA NA DIZEL MOTOR PRI KORIŠĆENJU HIBRIDNI BIODIZEL

Primarni cilj ove studije je da se naizmenično koriste konvencionalna fosilna goriva i smanji emisija gasova sa efektom staklene bašte i sumpor-dioksida iz dizel motora. Da bi se smanjila emisija NO_x, primenjena je tehnika recirkulacije izduvnih gasova (EGR) korišćenjem hibridnog alternativnog biodizela u tri različite proporcije od 5%, 10% i 15% pri optimalnom odnosu kompresije od 20:1. Rezultati pokazuju da za hibridni alternativni biodizel sa kompresijom od 20:1 i pod punim opterećenjem, toplotna efikasnost kočnice (BTHE) iznosi 31,8% sa 10% EGR. Sa 15% EGR, vršni pritisak za hibridni biodizel je niži nego što bi bio bez EGR-a za oko 2,28%. Kada se EGR poveća, kašnjenje paljenja i emisije NO_x se blago smanjuju. Sa povećanjem EGR samo do 10%, vrednosti potrošnje goriva specifične za kočnice (BSFC) se efikasno smanjuju. Hibridni biodizel sa 10% EGR smanjuje temperaturu izduvnih gasova na 341 °C.

Ključne reči: recirkulacija izduvnih gasova, sagorevanje, erformanse, emisija, ulje od otpadne plastike, kaučukuovo ulja.

NAUČNI RAD